Chemical Research in Toxicology

Article

pubs.acs.org/crt

Hepatic Metabolism of Carcinogenic β-Asarone

Alexander T. Cartus,[†] Simone Stegmüller,[†] Nadine Simson,[†] Andrea Wahl,[†] Sylvia Neef,[†] Harald Kelm,[‡] and Dieter Schrenk*[,†]

[†]Food Chemistry and Toxicology, University of Kaiserslautern, Erwin-Schroedinger-Strasse 52, 67663 Kaiserslautern, Germany

[‡]Inorganic Chemistry, University of Kaiserslautern, Erwin-Schroedinger-Strasse 52, 67663 Kaiserslautern, Germany

Supporting Information

ABSTRACT: β-Asarone (**1**) belongs to the group of naturally occurring phenylpropenes like eugenol or anethole. Compound **1** is found in several plants, e.g., *Acorus calamus* or *Asarum europaeum*. Compound **1**-containing plant materials and essential oils thereof are used to flavor foods and alcoholic beverages and as ingredients of many drugs in traditional phytomedicines. Although **1** has been claimed to have several positive pharmacological effects, it was found to be genotoxic and carcinogenic in rodents (liver and small intestine). The mechanism of action of carcinogenic ***allylic*** phenylpropenes consists of the metabolic activation via cytochrome P450 enzymes and sulfotransferases. *In vivo* experiments suggested that this pathway does not play a major role in the carcinogenicity of the ***propenylic*** compound **1** as is the case for other propenylic compounds, e.g., anethole. Since the metabolic pathways of **1** have not been investigated and its carcinogenic mode of action is unknown, we investigated the metabolism of **1** in liver microsomes of rats, bovines, porcines, and humans using ^{1}H NMR, HPLC-DAD, and LC-ESI-MS/MS techniques. We synthesized the majority of identified metabolites which were used as reference compounds for the quantification and final verification of metabolites. Microsomal epoxidation of the side chain of **1** presumably yielded (*Z*)-asarone-1′,2′-epoxide (**8a**) which instantly was hydrolyzed to the corresponding *erythro*- and *threo*-configurated diols (**9b**, **9a**) and the ketone 2,4,5-trimethoxyphenylacetone (**13**). This was the main metabolic pathway in the metabolism of **1** in all investigated liver microsomes. Hydroxylation of the side chain of **1** led to the formation of three alcohols at total yields of less than 30%: 1′-hydroxyasarone (**2**), (*E*)- and (*Z*)-3′-hydroxyasarone (**4** and **6**), with **6** being the mainly formed alcohol and **2** being detectable only in liver microsomes of Aroclor 1254-pretreated rats. Small amounts of **4** and **6** were further oxidized to the corresponding carbonyl compounds (*E*)- and (*Z*)-3′-oxoasarone (**5**, **7**). 1′-Oxoasarone (**3**) was probably also formed in incubations with **1** but was not detectable, possibly due to its rapid reaction with nucleophiles. Eventually, three mono-*O*-demethylated metabolites of **1** were detected in minor concentrations. The time course of metabolite formation and determined kinetic parameters show little species-specific differences in the microsomal metabolism of **1**. Furthermore, the kinetic parameters imply a very low dependence of the pattern of metabolite formation from substrate concentration. In human liver microsomes, 71−75% of **1** will be metabolized via epoxidation, 21−15% via hydroxylation (and further oxidation), and 8−10% via demethylation at lower as well as higher concentrations of **1**, respectively (relative values). On the basis of our results, we hypothesize that the genotoxic epoxides of **1** are the ultimate carcinogens formed from **1**.

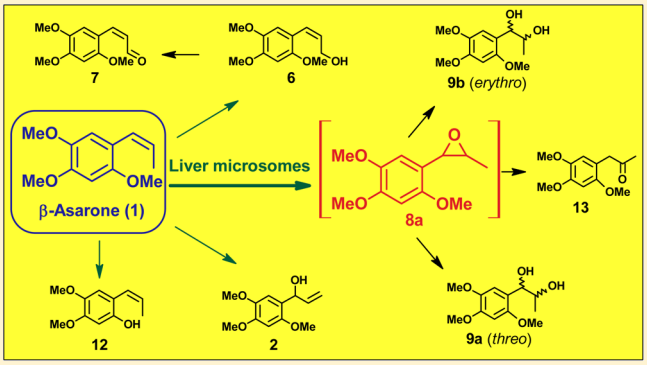

INTRODUCTION

β-Asarone (**1**, Scheme 1) belongs to the group of phenylpropenes (alkenylbenzenes) like eugenol, anethole, or safrol and is a known hepatocarcinogen to male mice. Compound **1** is found in plants of the genus *Acorus* (e.g., *A. calamus* L.; 'Sweet flag', *A. gramineus* SOL.) and *Asarum* (e.g., *A. europeaum* L.). The essential oil of the rhizome of Indian, tetraploidic *A. calamus* consists of up to 96% of **1**.[1,2] *A. calamus* is used in traditional phytomedicine of many ethnicities. Its dried rhizome is used to flavor alcoholic beverages like bitters and is consumed as tea.[3] Compound **1** and **1**-containing plant extracts are claimed to have multiple beneficial pharmacological actions, e.g., to act as a sedative, CNS depressant, anticonvulsant, antispasmodic, antidiarrheal, and anticholinergic drug.[4−6] Furthermore, ameliorative neuronal effects on memory disorder or learning performance are described in the literature.[4] Multiple reports on hallucinogenic effects of **1**-rich *A. calamus* after oral ingestion or after chewing or smoking its dried roots repeatedly led to acute poisonings in the past with prolonged vomiting being the main symptom. However, there is no scientific evidence for hallucinogenic properties of **1** or *A. calamus*.[7−9] Pharmacokinetic studies of **1** in rats and rabbits showed that orally administered **1** is rapidly absorbed in the gastrointestinal tract and is able to cross

Received: May 27, 2015

DOI: 10.1021/acs.chemrestox.5b00223
Chem. Res. Toxicol. XXXX, XXX, XXX−XXX

Scheme 1. Metabolic Pathways of β-Asarone (1) in Liver Microsomes of Different Species

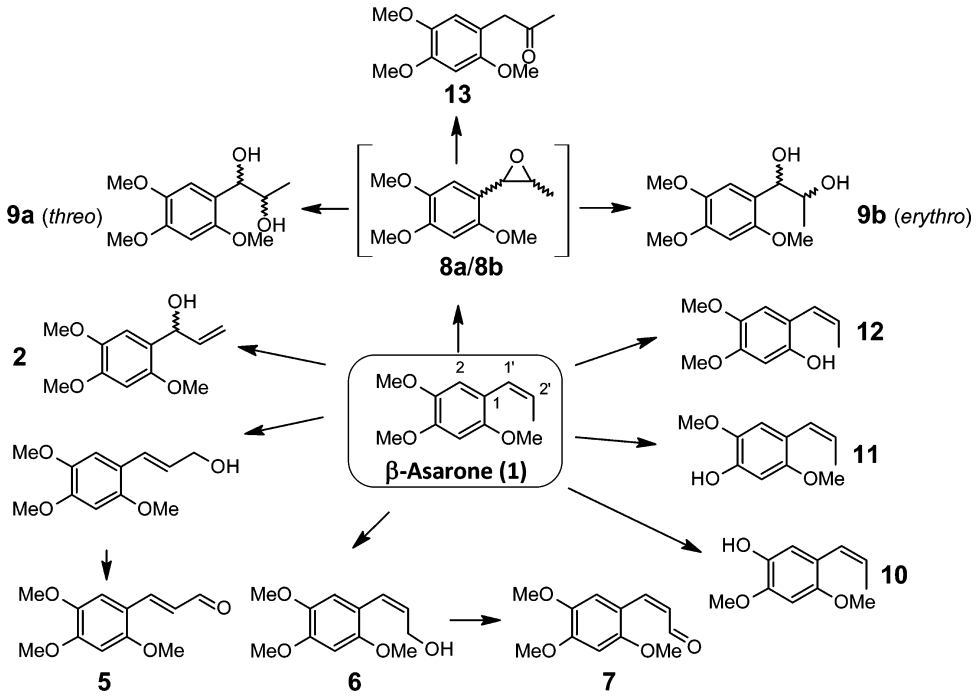

the blood−brain barrier.[10−12] The acute toxicity of **1** is low with LD_{50} values of 1 010 mg/kg body wt for rats (oral) and 184.2 mg/kg body wt for mice (ip). Subacute administration (100 mg/kg body wt, 5 days) caused weight loss, decreased specific heart and thymus weights, and increased kidney weights of preweanling Sprague−Dawley rats. Chronically, **1** (ip) induced hepatocellular adenomas and carcinomas in male C57BL/6J × C3H/HeJ F1 mice[13], whereas the carcinogenic effects of orally administered **1** in male and female rat livers were equivocal.[14] The mouse study included five different experiments with **1** given in repeated dosages (in sum 1 mg per animal) and single dosages of 52 and 104 mg/kg body wt with a total of 165 treated animals. Hepatoma incidences were reported to be between 62 and 94% with an average number of hepatomas per mouse of 1.1−2.3 (control animals: 9−17% hepatoma incidence with an average of 0.1−0.2 hepatomas/mouse). In male rats, **1** (0.04, 0.08, and 0.2% of **1** in the feed, 2-year study) resulted in increased mortality, and several pathological changes in the liver, kidney, and the small intestine (leiomyosarcomas) were observed.[14] For the latter effect, a benchmark dose lower confidence limit 10% ($BMDL_{10}$) of 9.6−21.5 mg/kg body wt per day was calculated.[15] Treatment of male and female rats with Indian calamus oil (0.5% in the feed, 2-year study) consisting of about 76% **1** and 3% α-asarone (the *trans*-configurated isomer of **1**, CAS No. 2883-98-9) resulted in several pathological degenerative and regenerative changes of the liver, cardiac fibrosis, and atrophy as well as leiomyosarcomas of the small intestine. In addition, hepatocellular adenomas and carcinomas (and other pathological findings) were observed in male and female rats fed with European calamus oil (0.1, 0.5, 1.0, 2.0% in the feed; composition unknown, 2-year study) (unpublished studies/abstract cited in more detail by JECFA, 1981 and SCF, 2002[14,16,17]). In Osborne−Mendel rats, growth was depressed, mortality increased, and liver and heart changes were observed after subchronical oral treatment with calamus oil.[17]

Wiseman et al. showed that the pretreatment of male mice with pentachlorophenol (PCP, ip), a potent inhibitor of sulfotransferases, had no effect on the incidences of hepatocellular adenomas and carcinomas caused by **1**.[13] Thus, a mechanism via side-chain hydroxylation, further sulfonation, and formation of a carbocation, which is the canonical mechanism of action of the activation of some ***allylic*** phenylpropenes, seems not to be responsible for the carcinogenicity of **1** as is the case for other ***propenylic*** phenylpropenes, e.g., anethole, which is claimed to be carcinogenic but nongenotoxic.[18] Nonetheless, (hepatic) metabolism seems to be necessary for bioactivation since **1** was found to be mutagenic in the Ames test (TA 100) only with metabolic activation.[19,20] Furthermore, **1** induced unscheduled DNA synthesis in primary rat hepatocytes,[21] increased the frequency of micronuclei in HepG2 cells, with but not without S9-mix,[22,23] and caused sister chromatid exchange in human lymphocytes with metabolic activation *in vitro*.[24] Because of the described toxicological properties of **1** (and at least to some extent also of α-asarone), the addition of *A. calamus*, calamus oil, or calamus extracts to food is prohibited within the U.S.,[25] and the direct use of **1** as a food flavoring is prohibited in Europe. Maximum levels for **1** in naturally flavored alcoholic beverages are set to a limit of 1 mg/kg in the EU.[26] Compound **1** and several essential oils of calamus were evaluated by JECFA in 1981,[14] SCF in 2002,[17] and the Council of Europe in 2005.[27] SCF came to the conclusion that **1** has a weak carcinogenic effect in rats and that a genotoxic potential cannot be ruled out.[17] In addition, the Council of Europe came to the conclusion that **1** is clearly carcinogenic to rodents and potentially genotoxic. Because of this, no ADI could be established, but it was recommended that calamus oil used in food should contain the lowest possible level of **1**. Human exposure to **1** resulting from foodstuffs seems to be relatively low (0.5−2.3 μg/d). Highest intakes are assumed to most likely arise from the consumption of alcoholic beverages flavored with *A. calamus* rhizome and preparations thereof. Assuming a daily consumption of 40−100 μL of alcoholic beverages containing the maximum limit of 1 mg/kg for **1**, the intake would be in the range of 20−100 μg/d. The total dietary intake of **1** via foods and alcoholic beverages was

DOI: 10.1021/acs.chemrestox.5b00223
Chem. Res. Toxicol. XXXX, XXX, XXX−XXX

estimated to be in the range of 8.5−49 μg/day for mean and high users.[27] However, due to the possible positive pharmacological effects mentioned above, calamus preparations are often used as ingredients in plant food supplements (PFS). Van den Berg et al. investigated different commercially available PFS and measured the amount of **1** therein.[15] Because of the recommended daily intake of the investigated PFS given by the suppliers, the daily intake of **1** was calculated to be 3−635 μg/kg body wt day. On the basis of these intakes and the above-mentioned $BMDL_{10}$ (leiomyosarcomas in male rats), the resulting margin of exposures (MoE) varied between 7 000 and 20 for **1** in the PFS. The authors concluded that **1**-containing PFS might raise a potential concern for human health and would be of high priority for risk management, at least if taken over a longer life-span and provided that no matrix effects would occur.

Although many pharmacological effects and suggestions for mode of actions of **1** are described in the literature, no data on the metabolism of **1** are yet available, and thus, nothing is known about its genotoxic/carcinogenic mechanism of action. SCF and COE stated the lack and need of studies with respect to this issue.[17,27] Therefore, we investigated the metabolism of **1** using rat, pig, bovine, and human liver microsomes and determined kinetic parameters of metabolite formation. To the best of our knowledge, this is the first study of the metabolism of a *cis*-configurated phenylpropene. Furthermore, the synthesis of compounds **2**, **3**, **6** (as well as its precursor 3-(2,4,5-trimethoxyphenyl)-2-propin-1-ol), and **8b** has not been reported so far.

EXPERIMENTAL PROCEDURES

Chemicals and Materials. Standard chemicals and solvents for the synthesis of metabolites were obtained in analytical grade or appropriate grade for the use intended by commercial suppliers and were used without further purification unless otherwise noted. Chemicals and enzymes for microsomal incubations were purchased from the following manufacturers: acetone, acetonitrile, ethyl acetate, and all salts were purchased from Merck (Darmstadt, Germany). β-NADP, glucose-6-phosphate, and glucose-6-phosphate dehydrogenase were obtained from Sigma-Aldrich/Fluka (Taufenkirchen, Germany). Methanol was obtained in HPLC gradient grade from Promochem (Wesel, Germany). Water was used double distilled and degassed (HPLC). Aroclor 1254 was originally purchased from Monsanto (St. Louis, MO, USA). 3,4-Dimethoxypropylbenzene (**14**) was synthesized according to the procedure previously described.[28] β-Asarone (**1**) was isolated from commercial essential oil of the rhizome of tetraploide indian *Acorus calamus* L. (Dragonspice Naturwaren, Reutlingen, Germany) as described in the synthesis section of the Supporting Information. Compounds **2**−**13** were synthesized using the methods described in the synthesis section of the Supporting Information as well. All consumables were purchased from Greiner Bio-One (Frickenhausen, Germany).

Analytical Methods. NMR spectra were recorded on a Bruker (Bruker BioSpin, Rheinstetten, Germany) Avance 200, Avance 400, or Avance 600 MHz spectrometer in DMSO-d_6 (^{1}H NMR: δ 2.49 ppm) at room temperature (294−298 K). Analysis was performed with 1D WIN-NMR or TopSpin (Bruker BioSpin, Rheinstetten, Germany). For clarity reasons, atom numbering for NMR signal assignment was not performed according to systematic names of the compounds according to the IUPAC rules but according to the assignment shown in Scheme 1 for β-asarone (**1**).

The LC-MS/MS system (for identification of metabolites) consisted of a PerkinElmer (Waltham, MA, USA) LC-system coupled to a triple quadrupole mass spectrometer (API 2000, PE SCIEX, USA). The MS was operated using an electrospray ionization source either in positive or negative ion mode (ESI^+/ESI^-). Acquisition and data processing were done with Analyst software, version 1.4 (Applied Biosystems, MDS SCIEX, USA). The "default" instrumental settings used for the MS were as follows: ion source temperature, 400 °C; declustering potential, 20 V; focusing potential, 200 V; entrance potential, 5.0 V; curtain gas, 20; ion source gas, 20; and turbo gas, 20 (the latter three are given in arbitrary units in the Analyst software). Fragmentation experiments were done with a collision-associated dissociation gas pressure of 5, a variable collision energy (CE 10−40 eV), and a cell entrance potential of 10.7 V.

Analytical HPLC was carried out using an Agilent 1200 HPLC system equipped with an autosampler (G1329A), a quadruple pumping system (G1311A), a diode array spectrophotometer (DAD G1315A), and a column heater (G1316A; Agilent, Waldkirch, Germany). HPLC and LC-MS/MS separations were performed using an RP18 column (Highbar, 5 μm, 4.0 mm × 125 mm, LiChrosorb, Merck, Darmstadt, Germany). The mobile phase system consisted of water (A) and MeOH (B). Separation was achieved using a 30 min linear gradient to 70% B from initial conditions of 10% B, following a 7 min period with constant eluent composition of 70% B with a total analysis time of 39 min per run at a flow-rate of 1 mL/min. The column temperature was kept constant at 35 °C. Detection (and reference) wavelengths were 230 (360), 261 (360), 280 (360), 310 (450), and 340 (450) nm. Injection volumes were 50 μL. Measuring and analysis were performed with ChemStation for LC 3D systems, version B03.02 (Agilent Technologies, Waldkirch, Germany). All chromatograms shown in this article and in the Supporting Information as well as all mentioned retention times of metabolites and reference compounds refer to measurements using this gradient and analytical conditions.

Preparative HPLC was performed with an Agilent 1200 series system comprising two preparative pumps (G1361A), an automatic fraction collector (G1364B), and a multiwavelength detector (G1315A). Injection was achieved over a manual valve with a 10.0 mL sample loop. As column, an RP18 (Reprosil 100, 5 μm, 250 × 20 mm; Dr. Maisch GmbH, Ammerbuch-Entringen, Germany) was used. Solvents were water (A) and methanol (B) with the following gradient: min 0−5 with an initial flow from 3 to a final flow of 15 mL/min at 40% B; min 5−30:40% B; min 30−55:40−55% B; min 55−65:55−90% B; min 65−70:90−40% B. The fraction collector was set to collect fractions every 1.0 min in the elution time of interest (min 15−45) to yield a fraction volume of 15 mL each. Detection wavelengths were the same as those used for analytical HPLC. Measuring and analysis were performed with ChemStation for LC systems, version B04.01 (Agilent Technologies, Waldkirch, Germany).

UV spectra of compounds sensitive to hydrolysis (**8a** and **8b**) were obtained in DMSO or MeCN using a NanoDrop ND-1000 spectrophotometer (ThermoScientific, Wilmington, NC, USA).

Microsomes. All animal experiments (rats) were performed according to national animal welfare regulations after authorization by the local authorities (Landesuntersuchungsamt Rheinland-Pfalz, Koblenz, Germany). Male Wistar rats were purchased from Charles River (Sulzbach, Germany) and Janvier Labs (Le Genest-Saint-Isle, France). Animals were kept under a 12 h light/dark cycle and received water and commercial laboratory chow ad libitum. For enzyme induction, rats (180 to 250 g body wt) were given a single dose of 500 mg/kg body wt Aroclor 1254 ip from a 200 mg/mL stock solution of Aroclor 1254 solved in corn oil. Five days after treatment, the animals were sacrificed. Liver microsomes of Aroclor 1254-pretreated rat, untreated/noninduced rat, bovine, and porcine origin were prepared from the livers of freshly sacrificed/slaughtered animals as described for rat livers in ref 29. Bovine livers were from healthy 1.5−2-year-old female German Black Pied cattle (dairy cattle) and were obtained from a local slaughterhouse. Porcine livers were from healthy female German pigs (hybrids from ♂ Piétrain × ♀ db. Viktoria) and were also obtained from a local slaughterhouse. Human liver microsomes were purchased from BD Bioscience (Heidelberg, Germany)/Corning Life Science (Kaiserslautern, Germany) as a pool derived from 150 mixed-gender donors. Protein concentrations were measured spectrophotometrically using the method of Bradford.[30] Total P450 contents were measured according to the method of Omura and Sato[31] and were found to be 1.34−1.67 (liver microsomes of Aroclor 1254-treated rats), 0.88 (bovine liver microsomes), 0.39 (porcine liver microsomes), 0.35 (human liver microsomes), and 0.28−0.34 (rat liver microsomes) nmol/mg protein.

DOI: 10.1021/acs.chemrestox.5b00223
Chem. Res. Toxicol. XXXX, XXX, XXX−XXX

Microsomal Incubations. Incubations of liver microsomes (1.0 mg of microsomal protein/mL final volume) were performed with varying substrate concentrations from a 100× stock solution in MeCN (final concentration 1%) with an NADPH-regenerating system (consisting of 1 mM NADPH, 0.5 unit/mL glucose-6-phosphate dehydrogenase, and 5 mM glucose-6-phosphate), 3 mM magnesium chloride, and 50 mM phosphate buffer (pH 7.4). Incubations were carried out in various volumes (from 100 μL to 100 mL for preparative uses) and were gently shaken in an incubator (TH-30; Carl Roth, Karlsruhe, Germany) at 37 °C. After preincubation with substrate for 5 min at 37 °C, the reactions were started by the addition of the NADPH-regenerating system, and the mixtures were incubated for up to 17 h. Control incubations were carried out with heat-inactivated microsomes and with intact microsomes but without the NADPH-regenerating system. The formation of NADPH in the NADPH-regenerating system was checked spectrophotometrically using a NanoDrop ND-1000 (ThermoScientific, Wilmington, NC, USA). All incubations were performed at least twice in independent experiments as indicated in the corresponding Figures or Tables.

Sample Preparation. After incubation, samples were diluted with equal volumes or 2:1 (v/v) of an ice-cold solution of acetone containing 0.1 or 0.5 mM **14** as internal standard. Samples were cooled for a minimum of 20 min on ice or at −20 °C. The mixtures were shaken vigorously, and the precipitated protein was removed by centrifugation (13 000*g*, 5 min). For time course measurements, the supernatants were used directly for HPLC analysis. Incubation suspensions of preparative experiments were extracted five times with an equal volume of ethyl acetate. The solvent of the combined organic phases was dried over anhydrous $MgSO_4$ and removed in vacuo, and the residue was dissolved in a defined volume of 90% methanol in water.

Identification of Metabolites Using ^{1}H NMR Spectroscopy. The methanolic solutions obtained after sample preparation of the preparative incubations were filtered (Nylon, 0,22 μm) and separated via preparative HPLC under the conditions mentioned above. Because of the used gradient, compounds in the particular fractions were now present in a mixture of different ratios of methanol and water. A small aliquot (100 μL) of each fraction was applied to the analytical HPLC to verify its composition. Fractions containing the same peaks were pooled and extracted three times with an equal volume of ethyl acetate. The combined organic phases were dried over $MgSO_4$, and the solvent was evaporated in vacuo at a temperature not greater than 30 °C. The residues of each (combined) fraction were dissolved in 250−350 μL of DMSO-d_6 and transferred into 3 mm (diameter) NMR tubes. Measurements were performed with a 600 MHz NMR spectrometer at room temperature (295−298 K).

Quantification of Metabolites. For quantification of the microsomal metabolites, the synthesized reference compounds were analyzed at different concentrations between 1 and 1000 μM in methanol with the HPLC gradient described above. Injection volumes were 50 μL each. Peak areas detected at five different wavelengths (λ = 230, 261, 280, 310, and 340 nm) were plotted versus concentration. Metabolite concentrations were calculated in relation to the internal standard from the slope of the linear regression ($r^2 \geq 0.99$ for each compound) at the most selective and sensitive wavelength for compounds **3**, **5**, and **7** (λ = 340 nm) or the most sensitive wavelength (λ = 230 nm) for all other compounds. 3,4-Dimethoxypropylbenzene (**14**) was used as internal standard.

Determination of Apparent Kinetic Parameters. Kinetic parameters were determined by incubating liver microsomes with the substrate at five different concentrations (50, 100, 200, 400, and 800 μM) for 20 min in a final volume of 100 μL under otherwise identical incubation conditions as described above (n = 2). Metabolite concentrations were calculated, converted into formation velocities [nmol product min^{-1} mg protein^{-1}] and plotted versus the substrate starting concentration. The Michaelis−Menten ($v = V_{max} \times [S]/(K_m+[S])$) and Hill equations ($v = V_{max} \times [S]^{nH}/(K_m{}^{nH}+[S]^{nH})$) in which $[S]$ represents the substrate concentration, V_{max} the maximum velocity, and K_m the Michaelis−Menten constant, and n_H the Hill coefficient for the formation of the different metabolites of **1**) were fitted to these data (OriginLab 8.0). Furthermore, Eadie−Hofstee diagrams (v vs $v/[S]$) were plotted to determine biphasic or other nonclassical kinetic profiles by visual inspection.[32] The quality of the fit to a particular model was determined by the evaluation of four criteria: (1) the randomness of the residuals; (2) the size of the sum of the squares of the residuals; (3) the standard error of the parameter estimates; and (4) the better coefficient of determination (r^2).[33] Apparent kinetic parameters are given ±SE provided from the fit for V_{max} and K_m. The errors for the quotients (V_{max}/K_m) are the fractional square root of the sum of the fractional squares of the SE in both operators in the case of Michaelis−Menten and Hill plots. In the case of Eadie−Hofstee plots, errors are propagated errors calculated with the SE of V_{max} and K_m.

RESULTS

Identification of Metabolites. Metabolites in the supernatants of microsomal incubations were identified via ^{1}H NMR spectroscopy, HPLC-DAD, and LC-UV-ESI-MS/MS. For this purpose, liver microsomes from Aroclor 1254-pretreated rats were incubated at a preparative scale with β-asarone (**1**, 1.2 mM) in a final volume of 100 mL for 10 h. After workup of the incubation suspension, a sample of the supernatant was analyzed by HPLC-DAD and LC-UV-ESI-MS/MS. Metabolites were then separated quantitatively via preparative HPLC, and selected (combined) fractions were analyzed by ^{1}H NMR spectroscopy. Figure 1 shows a representative set of (analytical) HPLC-DAD chromatograms of the incubation supernatant at different detection wavelengths. Four fractions (a−d) of the preparative incubation yielded sufficient amounts of material for the recording of meaningful NMR spectra. Compound **1** had a retention time of 28.7 min at the given conditions. The internal standard (3,4-dimethoxypropylbenzene, **14**) eluted at t_R = 31.5 min, a retention time where no other compounds were found to elute.

*Fraction **a**: Side-Chain Diols **9a** and **9b**.* The identity of the two side-chain diols **9a** (*threo*) and **9b** (*erythro*) was clearly proven by ^{1}H NMR spectroscopy. Figure 2 shows a detailed view of the ^{1}H NMR signals from fraction a of the incubation which allows a distinction between **9a** and **9b** together with the NMR spectra of the synthesized reference compounds. All other analytical data (retention time, UV/vis spectra, and mass signals; given in the Supporting Information) of both diols found in the incubations are identical to those of the reference compounds. In all incubations, the diols were found at a nearly constant ratio of 1:4 (**9b**/**9a**).

*Fraction **b**: Ketone **13** and Side-Chain Alcohols **2**, **4**, and **6**.* (*Z*)-3′-Hydroxyasarone (**6**) and 2,4,5-trimethoxyphenylacetone (**13**) were identified as the main metabolites in the ^{1}H NMR spectrum of fraction b of the supernatant from the incubation of liver microsomes from Aroclor 1254-pretreated rats with **1**. Figure 3 shows this spectrum together with the ^{1}H NMR spectra of synthesized **6** and **13**. HPLC analysis of the reference compounds revealed that **13** has a retention time of 18.2 min and **6** of 18.5 min, resulting in the assignment shown in Figure 1.

The ^{1}H NMR spectrum of fraction b shows also the presence of (*E*)-3′-hydroxyasarone (**4**) and 1′-hydroxyasarone (**2**) in minor concentrations. Integration of the NMR signals revealed that the relative amounts of the side-chain alcohols **2**, **4**, and **6** in this incubation of liver microsomes from Aroclor 1254-pretreated rats was 18%, 12%, and 70%, respectively. Figure 4 shows the detailed view of the ^{1}H NMR of fraction b and the spectra of synthesized **2** and **4**.

The three side-chain alcohols (**2**, **4**, and **6**) were found to coelute at a retention time of 18.5 min. Also, arbitrary mixtures of the synthetic compounds **2**, **4**, and **6** coelute as one peak at 18.5 min. Even under forced conditions, it was not possible to separate the nonshouldered signals of those three metabolites via HPLC. Because of the same mass signals of **2**, **4**, and **6**, a

DOI: 10.1021/acs.chemrestox.5b00223
Chem. Res. Toxicol. XXXX, XXX, XXX−XXX

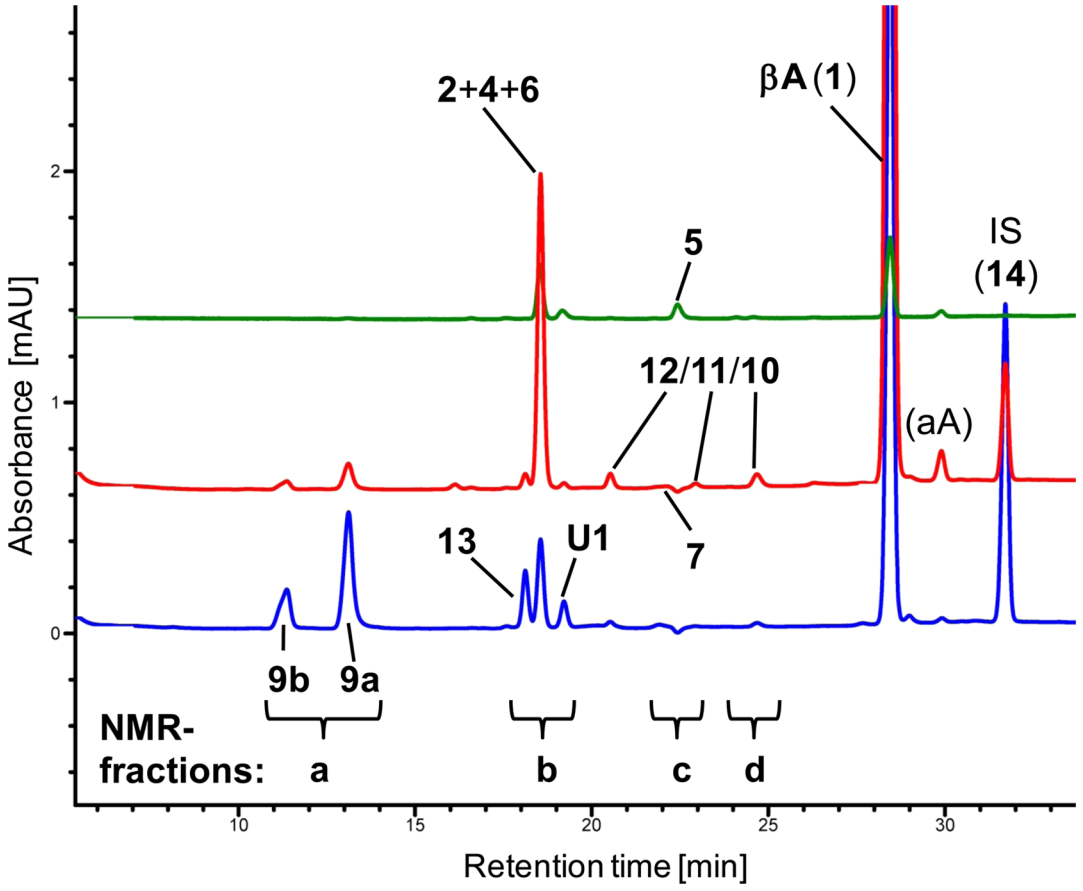

Figure 1. HPLC-DAD chromatograms and identified metabolites of the supernatant from an incubation of β-asarone (**1**, 400 μM) with liver microsomes from Aroclor 1254-pretreated rats (1 mg protein/mL) after 20 min of incubation time recorded at different detection wavelengths (reference wavelengths): bottom, λ = 280 nm (360 nm); middle, λ = 261 nm (360 nm); top, λ = 340 nm (450 nm). After separation via preparative HPLC, fractions a–d were subjected to ^{1}H NMR spectroscopy. aA, α-asarone; IS, internal standard **14**.

distinction of those metabolites via LC-MS/MS was not possible either. However, the UV spectrum of allylic compound **2** differs from those observed for propenylic compounds **4** and **6** (analytical data are presented in the Supporting Information). Therefore, we analyzed the UV spectra of the peaks resulting from different binary (**2** + **4** and **2** + **6**) and ternary (**2** + **4** + **6**) mixtures of the alcohols. These data show, that amounts of >5% of **2** in mixtures with **4** or **6** were detectable using the absorbance at λ = 290 nm compared to the absorbance at λ = 320 nm. At λ = 290 nm, **2** has an absorption maximum, and **4** and **6** have a local minimum of absorption in this range. Compound **4** has a maximum at λ = 315 nm and **6** at λ = 304 nm, whereas **2** shows no significant absorption in this region. Eventually, the amount of allylic **2** in the side-chain alcohol peaks at t_R = 18.5 min was calculated to be less than 20% for all incubations with liver microsomes from Aroclor 1254-pretreated rats and less than 5% (i.e., not detectable) for all incubations with other microsomes. Quantification of the three compounds was, therefore, accomplished as the sum of **2** + **4** + **6**, using a combined extinction coefficient, which considered the percentage contribution of the side-chain alcohols as it was found in the NMR spectrum (Figures 3 and 4) for the incubation of liver microsomes from Aroclor 1254-pretreated rats with **1**. The concentration of side-chain alcohols in all other incubations (i.e., with rat, bovine, porcine, and human liver microsomes) was estimated using a combined extinction coefficient considering a percentage contribution of 0%, 20%, and 80% for **2**, **4**, and **6**, respectively. Because of the different absolute extinction coefficients of **4** and **6** compared to **2** at the most sensitive wavelength (λ = 230 nm), this method will result in slightly lower numbers for the concentration of side-chain alcohols if the percentage of **2** is higher (0% < **2** < 5%) than estimated.

In order to determine the origin of ketone **13**, we investigated the spontaneous hydrolysis of both epoxides, **8a** and **8b**, at various pH-values (determined via HPLC-DAD, Figure S11). Although both synthesized epoxides were stable for several weeks in anhydrous organic solvents (dried DMSO-d_6, CD_3CN, and $CDCl_3$), the stability in an aqueous environment was very low. In ^{1}H NMR experiments, both epoxides (1 mM in D_2O, prepared freshly from a 0.1 M solution in DMSO-d_6) were quantitatively converted into the diols **9a** and **9b** and into ketone **13** in less than 4 min (the time which is needed for preparing the aqueous solution and measure a ^{1}H NMR spectrum with 8 scans). Under the same conditions as in the microsomal incubations but without protein (i.e., potassium phosphate buffer/$MgCl_2$, pH 7.4), 5.1 ± 1.3% of **8a** and 16.0 ± 0.5% of **8b** were converted to ketone **13**. The ratio of *erythro*- to *threo*-diol (**9b**:**9a**) was about 1:4 for both epoxides.

*Fraction c: Oxo Compounds **3**, **5**, and **7**.* The ^{1}H NMR spectrum of fraction c eluting between t_R = 21.5–23.0 min showed that (*E*)-3′-oxoasarone (**5**) and (*Z*)-3′-oxoasarone (**7**) are the main microsomal oxidation products of the side-chain alcohol metabolites **2**, **4**, and **6** in the β-asarone incubations (Figure S2). No NMR signals of 1′-oxoasarone (**3**) were

DOI: 10.1021/acs.chemrestox.5b00223
Chem. Res. Toxicol. XXXX, XXX, XXX–XXX

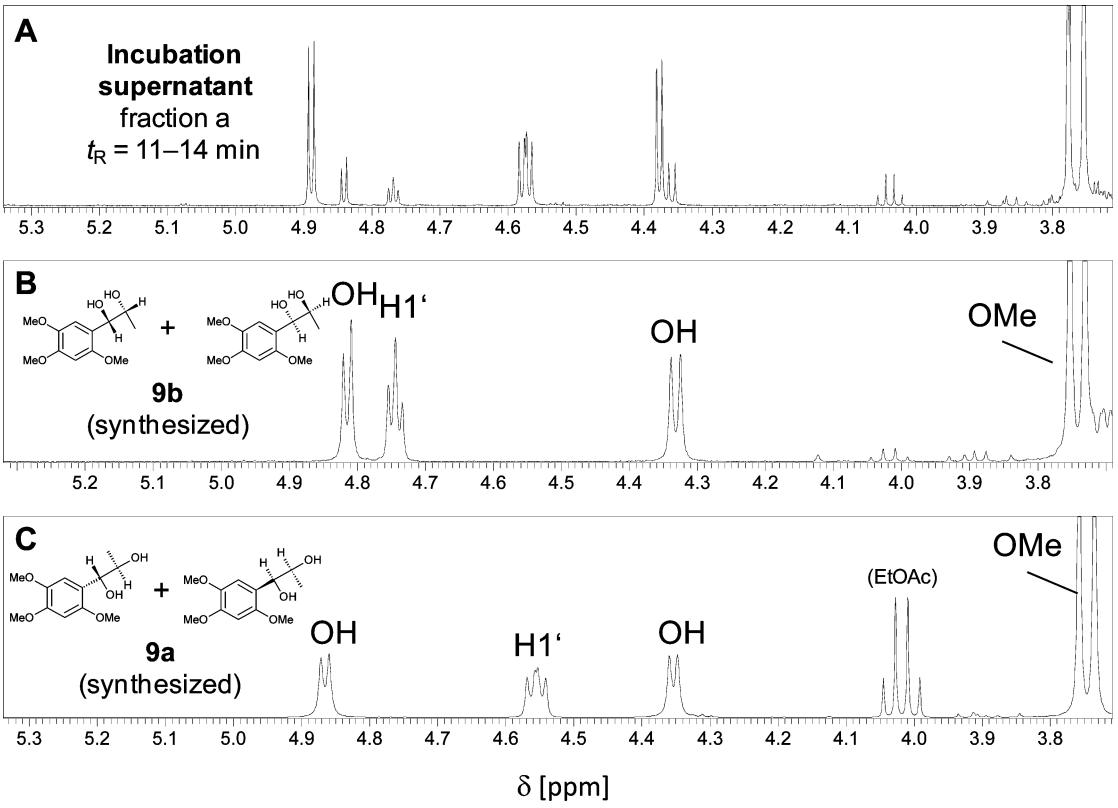

Figure 2. ^{1}H NMR spectra (details from δ = 3.7−5.3 ppm) of (A) the supernatant of the incubation of **1** with Aroclor 1254-pretreated rat liver microsomes (fraction a) eluting between minutes 11−14, (B) synthetic *erythro*-1′,2′-dihydrodihydroxy-asarone (**9b**), and (C) synthetic *threo*-1′,2′-dihydrodihydroxy-asarone (**9a**). All spectra were recorded in DMSO-d_6 at 295 K. Spectrum A was recorded at 600 MHz and spectra B and C at 400 MHz. The full scale spectra are shown in Figure S1.

detected in this spectrum. To get a deeper insight into the secondary metabolism of **2**, **4**, and **6**, we investigated their microsomal oxidation in separate incubations with liver microsomes from Aroclor 1254-pretreated rats (Figure S3). Incubation of **4** revealed one single new peak (t_R = 22.5 min), which could be identified as **5**. Incubations of **6** resulted in the formation of two new peaks with retention times of t_R = 22.5 and 21.9 min, identified as **5** and **7**, respectively. Both peaks had UV spectrum characteristics for α,β-unsaturated compounds and similar mass signals compared to those of the reference compounds. Incubation of **2** yielded a small amount of 1′-oxoasarone (**3**). Quantitatively, the extent of microsomal oxidation of the side-chain alcohols relative to **4** (= 100%) was about 10% for **6** and roughly 1% for **2**. In all incubations, **5** was found at the highest concentrations, followed by smaller amounts of **7**, whereas **3** was not detectable in any incubation of liver microsomes with **1**.

*Fractions **c** and **d**: Mono-O-demethylated Metabolites **10**, **11**, and **12***. The peaks with retention times of t_R = 20.7, 23.1, and 24.8 min were tentatively identified as the mono-*O*-demethylated compounds **10**, **11**, and **12**. All peaks showed identical UV spectra (λ_{max} = 250 and 302 nm) indicative of an unsaturated *cis*-configurated side-chain. The NMR spectra of fraction c (t_R = 21.5−23 min, Figure S4) and fraction d (t_R = 23.5−25 min, Figure S5) bear consistent signals (i.e., correct ratios of the signal integrals) of one phenolic proton at δ = 8.98 and 9.09 ppm, respectively, in addition to two signals of aromatic protons and two instead of three methoxy groups. This is a strong indication of the formation of mono-*O*-demethylated compounds from **1**. However, recording an NMR spectrum of the peak at t_R = 20.7 min was not successful. Because of the low amounts of these three metabolites in the incubations and the generally poor ionization of similar phenolic compounds using electrospray ionization in either positive or negative mode, no meaningful mass signals were observed. Comparison of the retention times of other related compounds with an unsubstituted side-chain (e.g., α-asaron and **1** or *trans*- and *cis*-methylisoeugenol) showed that the *cis*-isomer eluted 0.5−1.4 min earlier than the *trans*-isomer. Actually, the retention time of (*E*)-6-hydroxymethylisoeugenol (which is the *trans*-configurated isomer of **12**) was t_R = 21.5 min (Δt_R = 0.8 min) under the same chromatographic conditions. On the basis of this observation and the retention times of further monophenylic derivatives,[28] the following assignment is most likely: t_R = 20.7 min **12**, t_R = 23.1 min **11**, and t_R = 24.8 min **10**. This assumption is supported by the calculated ^{1}H NMR signals (calculated for a $CDCl_3$ solution with ChemDraw Ultra 10.0, CambrigeSoft), which predicts a phenolic singlet at δ = 9.48 ppm for **10** and **11** each (found: 8.98 and 9.09 ppm), and a signal at δ = 11.85 ppm for **12**.

Unidentified Peak at t_R = 19.1 min. In all incubations, a yet unidentified compound at t_R = 19.1 min was detected. On the basis of the detected LC-UV-ESI$^+$-MS signal, we assume a compound with a molecular weight of 226 g/mol. The peak had significant mass signals at m/z = 249.4 and 265.3 (most likely adducts with Na^+ and K^+) and two weaker signals at m/z = 227.3 and 209.2 (most likely $[M + H]^+$ and $[M + H - H_2O]^+$, respectively). The UV spectrum showed bands at λ = 230 (1), 285 (0.55), and 350 (0.19) nm (relative absorbance), which may be indicative of an α,β-unsaturated compound. However, a final identification of this compound was not successful since in the ^{1}H NMR spectrum of fraction b, no other significant signals aside

DOI: 10.1021/acs.chemrestox.5b00223
Chem. Res. Toxicol. XXXX, XXX, XXX−XXX

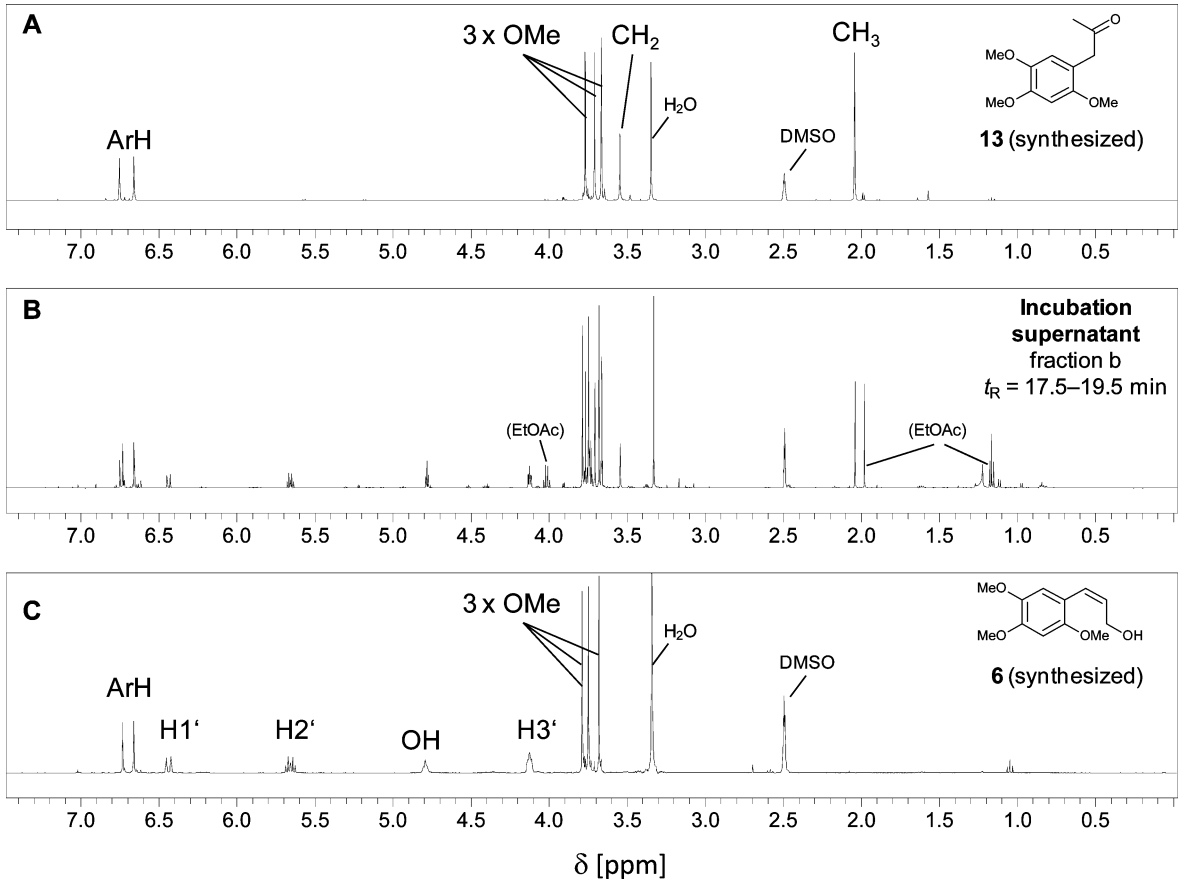

Figure 3. [1]H NMR spectra of (A) synthesized 2,4,5-trimethoxyphenylacetone (**13**), (B) the incubation supernatant of **1** with Aroclor 1254-pretreated rat liver microsomes eluting between minutes 17.5−19.5 (fraction b), and (C) (*Z*)-3′-hydroxyasarone (**6**). All spectra were measured in DMSO-d_6 at 295 K. Spectrum B was recorded at 600 MHz, and spectra B and C at 400 MHz.

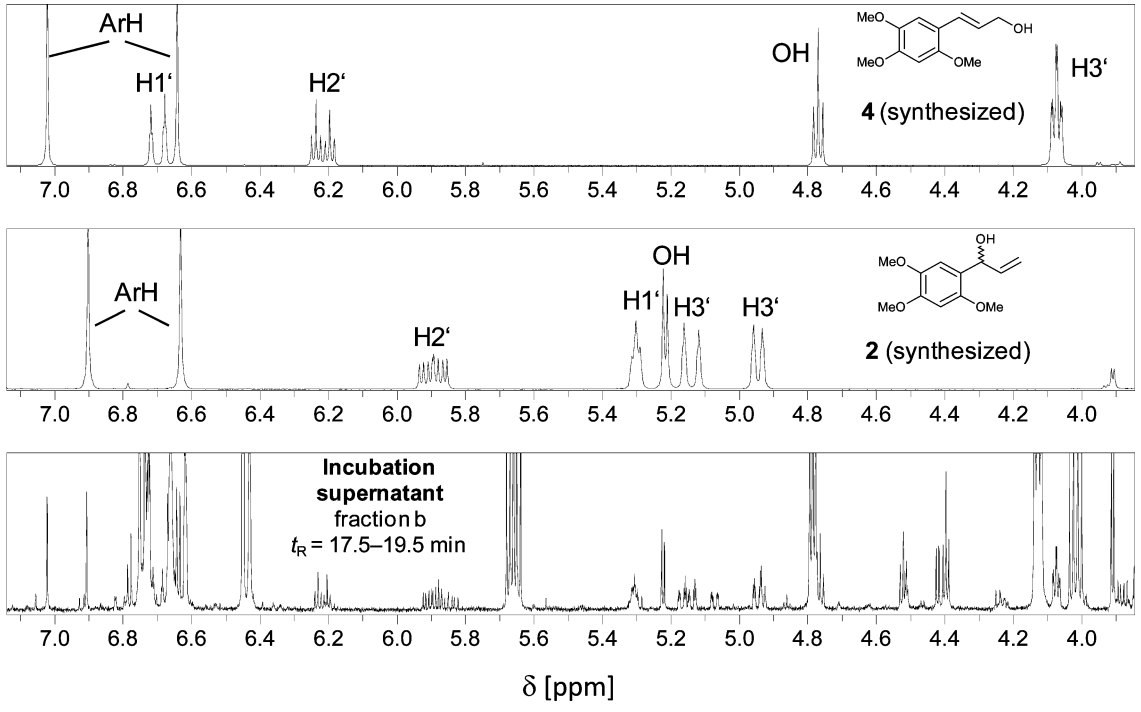

Figure 4. [1]H NMR spectra (δ = 3.9−7.1 ppm) of (top) synthetic (*E*)-3′-hydroxyasarone (**4**), (middle) synthetic 1′-hydroxyasarone (**2**), and (bottom) detailed view (zoomed *y*-axis) of the same spectra as shown in Figure 3B (fraction b). All spectra measured in DMSO-d_6 at 295 K. Top and middle spectra were measured at 400 MHz and the bottom spectrum at 600 MHz.

DOI: 10.1021/acs.chemrestox.5b00223
Chem. Res. Toxicol. XXXX, XXX, XXX−XXX

from the already assigned signals remained. Because of its similar spectroscopic properties, the concentrations of this metabolite in microsomal incubations were calculated using the extinction coefficient of **3**. On the basis of these results, the metabolic pathways of **1** in different liver microsomes are depicted in Scheme 1.

Time Course of Metabolite Formation. For time course measurements, substrate concentration in the middle range (500 μM) of those used for kinetic investigations (see below) and a protein concentration of 1 mg/mL were chosen. The aim was to identify an appropriate time point for the kinetic measurements where the formation rate of metabolites is short enough to be linear over time but long enough to produce sufficient (quantifiable) amounts of metabolites. We investigated six time points between 1 and 120 min as well as one late time point after 17 h, and liver microsomes of Aroclor 1254-pretreated rat, untreated rat, bovine, porcine, and human origin. In control incubations with heat-inactivated microsomes or without an NADPH-generating system, no quantifiable amounts of metabolites were detected (data not shown).

Figure 5 shows the results of these incubations with different liver microsomes. Selected sets of HPLC-DAD chromatograms of those experiments are shown in Figures S6–S10.

Corresponding to their high P450 amount, liver microsomes from Aroclor 1254-pretreated rats were most active in metabolizing β-asarone (**1**) in terms of final metabolite concentrations. The dominating pathway in all investigated microsomes was the formation of the side-chain diols **9a** and **9b**, and ketone **13**. In liver microsomes from Aroclor 1254-pretreated rats, 26% of the initial concentration of **1** was metabolized over this route during an incubation time of 1 h, and in sum, 15% was metabolized to the side-chain alcohols **2** + **4** + **6**. Small amounts (0.7%) of the oxidation products **5** + **7** were quantifiable as well as the sum of *O*-demethylated products **10** + **11** + **12** (1.6%) after 1 h. The highest concentrations of the yet unidentified metabolite **U1** were detected also in incubations with liver microsomes from Aroclor 1254-pretreated rats (appr. 2.7%). The metabolite concentrations in incubations with rat liver microsomes early reached a plateau (appr. after 40 min), after which the concentrations of the detectable metabolites did not significantly changed. Main metabolites in rat liver microsomes were the diols **9a** + **9b** and ketone **13** as was the case in all other incubations. In contrast to the other liver microsomes, oxidation leading to **5** + **7** was not quantifiable in incubations with rat liver microsomes. The qualitative patterns of metabolites in the other investigated liver microsomes (porcine, bovine, and human) did not significantly differ from those observed for liver microsomes from Aroclor 1254-pretreated rats, but the yields were lower. The ratios of **13**/(**9a** + **9b** + **13**) were highest at the beginning of all incubations and subsequently decreased continuously, e.g., in Aroclor 1254-pretreated rat liver microsomes from 27.5% (10 min) to 17.3% (2 h). Also, the ratio of *erythro*- to *threo*-diol (**9b**/**9a**) was roughly constant at 1:4 in all incubations at all time points. The overall ranking of metabolite yield was Aroclor 1254-pretreated rat liver microsomes > human liver microsomes > bovine liver microsomes > procine liver microsomes > rat liver microsomes/ and the formation rates for all metabolites were virtually linear with time over the first 25 min of incubation. Therefore, an incubation time of 20 min was chosen for the determination of kinetic parameters.

Kinetic Parameters. To determine apparent kinetic parameters, **1** was incubated with the different investigated liver microsomes (1 mg protein/mL) in concentrations between 50 and 800 μM over a period of 20 min together with an NADPH-generating system. Metabolite formation rates were plotted versus substrate start concentration and the Michaelis–Menten and Hill equations were fitted to the data. To uncover atypical kinetic profiles, Eadie–Hofstee diagrams were plotted as well. The plots are shown in Figures S12–S17. The derived data of V_{max}, K_m, and the calculated V_{max}/K_m values are apparent values, which are not mentioned each time when presented and discussed in the following text. The values are given in Table 1.

The majority of reaction kinetics were well characterized using the Michaelis–Menten or Hill equation. Certain biphasic or other atypical reaction profiles were observed by visual inspection of the Eadie–Hofstee plots for the formation of the sum of side-chain alcohols **2** + **4** + **6** in the incubations with bovine, porcine, and human liver microsomes, and for the formation of the sum of *O*-demethylated compounds, **10** + **11** + **12** in the incubations with bovine liver microsomes. The parameters for these reactions given in Table 1 are the ones obtained for the low K_m site.

The reactions with the highest V_{max} values in all investigated liver microsomes were the formation of the diols **9a** + **9b** and ketone **13**. Also, the highest V_{max}/K_m values were observed for these reactions with the exception of porcine liver microsomes, where the *O*-demethylation leading to **10** + **11** + **12** was highest due to the low K_m value for this reaction. To get a clearer picture, these data were further transformed into percentage values (V_{max} or V_{max}/K_m of one particular metabolite divided by the sum of V_{max} or V_{max}/K_m of all metabolites), which are given in Table 2. The V_{max} % values may be interpreted as the metabolite pattern in the case of high substrate concentrations, and the V_{max}/K_m % values may be interpreted as the metabolite pattern in the case of very low substrate concentrations.

The data show that the pattern of metabolites is nearly independent from the substrate concentration in the case of Aroclor 1254-pretreated rat, rat, bovine, and human liver microsomes. Only in porcine liver mircosomes the level of mono-*O*-demethylated metabolites seems to be higher at low substrate concentrations at the expense of the levels of the diols **9a** + **9b** and ketone **13**. The levels of the sum of ketone **13** + diols **9a** and **9b** allowed a calculation between V_{max} % = 84 and V_{max}/K_m % = 32 in porcine liver mircosomes, and between 68–84% in terms of V_{max} % and V_{max}/K_m % for all other investigated liver microsomes. The levels of the side-chain alcohols **2** + **4** + **6** were between 9% and 27% for all liver microsomes, and O-demethylation was a minor pathway in all liver microsomes with up to 10% with the exception of porcine liver microsomes at low substrate concentrations (V_{max}/K_m % = 52).

DISCUSSION

Identification of Metabolites. The side-chain diols **9a** (*threo*) and **9b** (*erythro*) were identified as the main metabolites in all incubations of liver microsomes with β-asarone (**1**). To a smaller extent, concomitant formation of ketone **13** was observed. Most likely, the corresponding *Z*-configurated epoxide **8b** is the precursor of both, diols and ketone, since **1** is *Z*-configured, and P450 catalyzed epoxidations occur most often in a *syn*-selective manner under retention of the stereostructure. However, it is generally agreed that the mechanism of olefin epoxidation by P450 enzymes is a nonconcerted stepwise process and can proceed also under partial or complete inversion.[34−36] Therefore, the intermediate formation of **8a** cannot entirely be ruled out. Mohan et al. investigated the formation of the ketone species and the ratio of *erythro*- and *threo*-diols in the

DOI: 10.1021/acs.chemrestox.5b00223
Chem. Res. Toxicol. XXXX, XXX, XXX−XXX

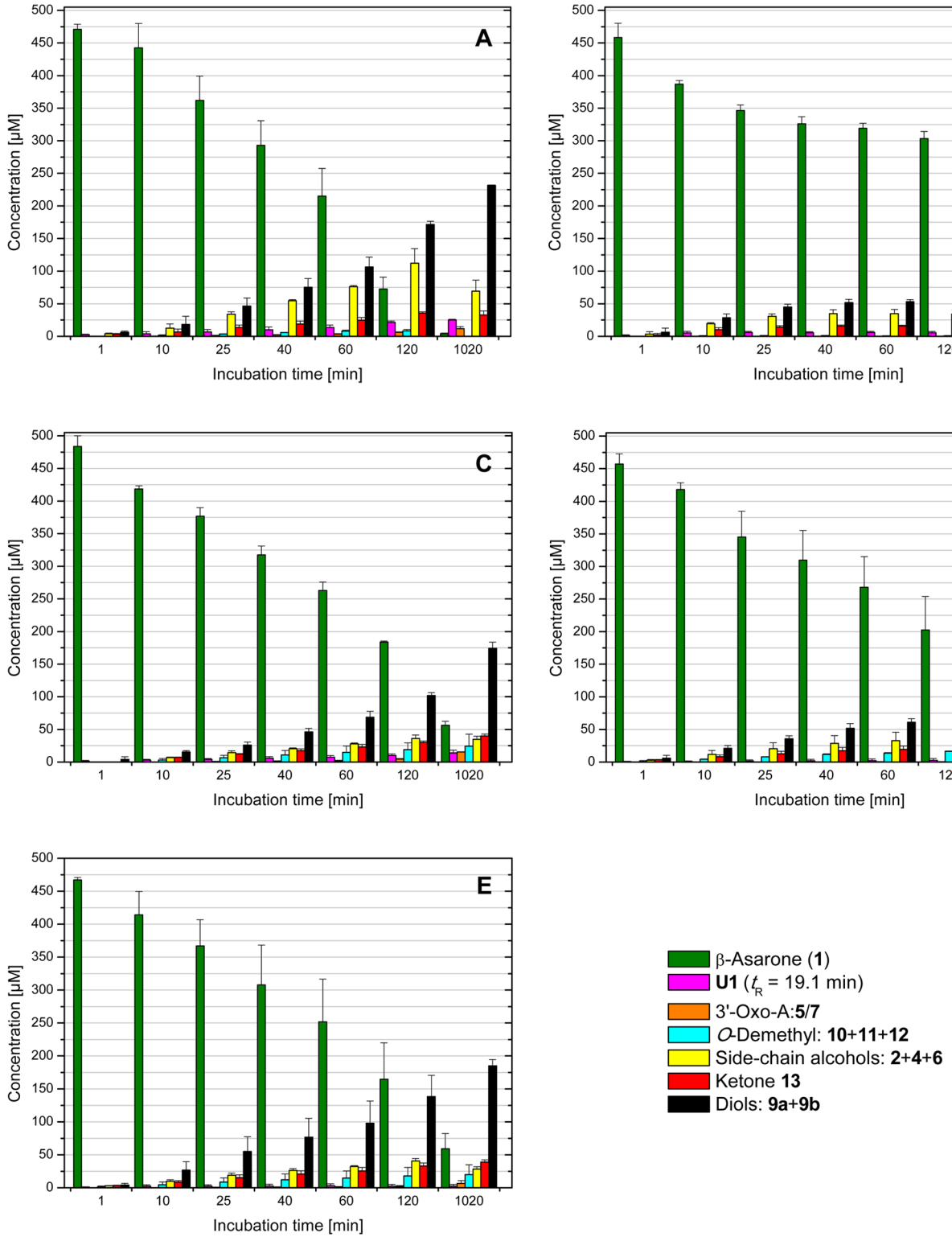

Figure 5. Quantification of metabolite levels during the incubation of liver microsomes with *β*-asarone (**1**). (A) Aroclor 1254-pretreated rat, (B) rat, (C) bovine, (D) porcine, and (E) human liver microsomes. Initial concentration of **1** was 500 μM. Values are the means ± SD from three independent incubations for human and porcine liver microsomes, means ± range from two independent incubations for Aroclor 1254-pretreated rat, rat, and bovine liver microsomes.

nonenzymatic hydrolysis of *cis*- (CAS No. 69262-97-1) and *trans*-anethole-epoxide (CAS No. 50618-02-5).[37] They found that the formation of the ketone as well as the ratio of *erythro*- and *threo*-diol was strongly dependent on the pH-value. Therefore, we investigated the hydrolysis of both asarone epoxides. In phosphate buffered water (pH 7.4), the conversion of **8a** and **8b** was quantitative and yielded 5.1% and 16.0% of ketone **13**, respectively. The ratio of *erythro*- to *threo*-diol (**9b**/**9a**) was about 1:4 for both epoxides. In microsomal incubations, the ratio of **13**/(**9a** + **9b** + **13**) was highest (>24%) at the beginning of all

DOI: 10.1021/acs.chemrestox.5b00223
Chem. Res. Toxicol. XXXX, XXX, XXX−XXX

Table 1. Apparent Kinetic Data of the Metabolite Formation from β-Asarone (1) in Different Liver Microsomes[a]

liver microsomes/apparent kinetic parameter	metabolite: side-chain alcohols (2 + 4 + 6)	3′-Oxo-A (5 + 7)	ketone (13)	diols (9a + 9b)	O-demethyl-asarones (10 + 11 + 12)
Aroclor 1254-Pretreated Rats					
V_{max} [nmol min^{-1} (mg protein)$^{-1}$]	0.99 ± 0.02[c]	0.06 ± 0.01[b]	0.93 ± 0.01[c]	2.37±0.12[c]	0.49 ± 0.09[b]
K_m [μM]	58 ± 2.5	nc	74 ± 2.2	49 ± 3.9	484 ± 158
V_{max}/K_m [nmol min^{-1} (mg protein) $^{-1}$ μM^{-1}]	17 ± 1.9		12 ± 1.6	49 ± 4.8	1.0 ± 0.4
Rat					
V_{max} [nmol min^{-1} (mg protein)$^{-1}$]	2.15 ± 0.28[c]	nd	1.61 ± 0.28[c]	4.13 ± 0.40[b]	0.16 ± 1.3 × 10^{-12}[c]
K_m [μM]	275 ± 70		210 ± 76	163 ± 32	399 ± 0.02
V_{max}/K_m [nmol min^{-1} (mg protein) $^{-1}$ μM^{-1}]	7.8 ± 2.4		7.7 ± 2.0	25 ± 5.3	0.4 ± 0.2
Bovine					
V_{max} [nmol min^{-1} (mg protein)$^{-1}$]	0.65 ± 0.05[d]	nd	1.49 ± 0.10[b]	2.27 ± 0.10[b]	0.17 ± 0.004[d]
K_m [μM]	92 ± 17		224 ± 31	85 ± 11	47 ± 3.2
V_{max}/K_m [nmol min^{-1} (mg protein) $^{-1}$ μM^{-1}]	7.1 ± 1.9		6.7 ± 1.7	27 ± 3.5	3.6 ± 0.3
Porcine					
V_{max} [nmol min^{-1} (mg protein)$^{-1}$]	0.54 ± 0.03[d]	nd	1.71 ± 0.20[b]	3.21 ± 0.20[b]	0.40 ± 0.01[b]
K_m [μM]	170 ± 13		920 ± 163	685 ± 58	38 ± 6
V_{max}/K_m [nmol min^{-1} (mg protein) $^{-1}$ μM^{-1}]	3.2 ± 0.4		1.9 ± 1.0	4.7 ± 2.2	11 ± 0.7
Human					
V_{max} [nmol min^{-1} (mg protein)$^{-1}$]	0.75 ± 0.07[d]	nd	1.13 ± 0.18[b]	2.61 ± 0.43[b]	0.49 ± 0.07[b]
K_m [μM]	281 ± 41		473 ± 130	389 ± 95	447 ± 115
V_{max}/K_m [nmol min^{-1} (mg protein) $^{-1}$ μM^{-1}]	2.7 ± 0.6		2.4 ± 1.0	6.7 ± 2.5	1.1 ± 0.4

[a]Values are obtained by different models (indicated by the V_{max} value). nd, not detectable; nc, not calculated (due to the lack of dose-dependence and thus nonreal K_m values). [b]Michaelis–Menten. [c]Hill. [d]The reaction was biphasic (values given for the low K_m site). The particular kinetic plots are shown in Figures S12–S17.

Table 2. Kinetic Data from Table 1 Expressed as Percentages

liver microsomes	apparent kinetic parameter[a]	metabolite: side-chain alcohols (2 + 4 + 6)	3′-Oxo-A (5/7)	ketone (13)	diols (9a + 9b)	O-demethyl-asarones (10 + 11 + 12)
Aroclor 1254-pretreated rat	V_{max} %	20	1	19	49	10
	V_{max}/K_m %	22	nc	16	62	1
rat	V_{max} %	27	0	20	51	2
	V_{max}/K_m %	19	0	19	61	1
bovine	V_{max} %	14	0	33	50	4
	V_{max}/K_m %	16	0	15	61	8
porcine	V_{max} %	9	0	29	55	7
	V_{max}/K_m %	16	0	9	23	52
human	V_{max} %	15	0	23	52	10
	V_{max}/K_m %	21	0	19	52	8

[a]V_{max} %, V_{max} of metabolite *i* divided by the sum of V_{max} of all metabolites; V_{max}/K_m%, V_{max}/K_m of metabolite *i* divided by the sum of V_{max}/K_m of all metabolites; nc, not calculated (due to the high K_m-value).

incubations and subsequently decreased continuously, e.g., in Aroclor 1254-pretreated rat liver microsomes from 27.5% (10 min) to 17.3% (2 h). Because of these high yields of **13** found in the microsomal incubations, the predominant formation of the *Z*-configured epoxide **8b** and subsequent concurrent spontaneous and enzymatic hydrolysis by microsomal epoxide hydrolase, rather than the formation of higher amounts of **8a**, are hence most likely.

Both epoxides **8a** and **8b**, as well as the diols **9a** and **9b**, are diastereoisomers to each other and chiral, thus forming two enantiomers. Because of the mechanism of the synthesis route, the synthesized expoxides and diols **8a**, **8b**, **9a**, and **9b** will be racemic. Experiments to determine whether one enantiomer of either **8a** and **9a** (1′*R*,2′*R* or 1′*S*,2′*S*) or **8b** and **9b** (1′*S*,2′*R* or 1′*R*,2′*S*) was formed preferentially in microsomal incubations were not feasible (epoxides) or not performed (diols). The half-life of both epoxides, **8a** and **8b**, in aqueous solutions was very low. For **8a**, Kim et al. reported a half-life of 4.0 min (0.1 M potassium buffer at pH 7.4) and 2.4 min (buffer +154 mM KCl) in an acetone/H_2O (1:2) solution using the 4-(4′-nitrobenzyl)pyridine-assay which is roughly in accordance with our findings.[38]

The detection of three side-chain alcohols, (*Z*)-3′-hydroxyasarone (**6**), (*E*)-3′-hydroxyasarone (**4**), and 1′-hydroxyasarone (**2**) in the incubations of Aroclor 1254-pretreated rat liver microsomes with **1** was somewhat surprising. Their formation

DOI: 10.1021/acs.chemrestox.5b00223
Chem. Res. Toxicol. XXXX, XXX, XXX–XXX

could clearly be proven via ^{1}H NMR spectroscopy. However, all three alcohols coeluated in one peak at t_R = 18.5 min, and several chromatographic attempts to separate these alcohols were not successful. Also, all three compounds are isobaric and generate the same LC-ESI-MS/MS mass signals. Though, the amount of **2** in different mixtures of **2** + **4** + **6** could be estimated only via HPLC-DAD using the different spectroscopic properties of the allylic (**2**) and propenylic (**4** and **6**) metabolites. The determination of the ratios of metabolites **4**:**6** in those mixtures failed due to the very similar UV spectra of both compounds. Amounts >5% of **2** (percentage of the sum of **2** + **4** + **6**) were just detected in incubations with Aroclor 1254-pretreated rat liver microsomes but not with the other investigated liver microsomes.

Although we have no mechanistic explanation for the formation of the allylic alcohol **2** in incubations of Aroclor 1254-pretreated rat liver microsomes with **1**, the *cis*-configuration of the double-bond in the side-chain of **1** seems to be crucial for its formation. In the case of *trans*-configured propenylic phenylpropenes like methylisoeugenol,[28,39] anethole,[40] isoelemicin,[41] and α-asarone (unpublished data), the formation of an allylic alcohol was not observed. Other studies (beside the here presented study) on the metabolism of a *cis*-configurated phenylpropene are, to our knowledge, not available. A nonenzymatical conversion or rearrangement of **6** into **4** or **2**, e.g., in aqueous solutions or during HPLC-analysis, was not observed in control experiments with synthesized **6** within the mentioned analytical limitations but could not be entirely ruled out.

The side-chain alcohols **2**, **4**, and **6** were found to undergo further enzymatic oxidation yielding the corresponding α,β-unsaturated ketone **3** or aldehydes **5** and **7**, respectively. (*E*)-3′-Oxoasarone was the oxo-compound found at highest levels, whereas **7** was only quantifiable in small concentrations (about 10% of **5**). This was surprising because the precursor of **7**, alcohol **6**, was the alcohol found in the highest concentrations in our incubations. Further experiments with **2**, **4**, and **6** as substrates showed that the observed formation of **3** from **2** in incubations of liver microsomes from Aroclor 1254-pretreated rats was lowest (Figure S3). The apparent formation of **7** (from **6**) and **5** (from **4**) was 10 and 100 times higher than that found for the formation of **3** from **2**. However, the oxo-compounds are reactive metabolites which probably form (Michael) adducts with the microsomal protein or residual glutathione present in the microsomal preparations with ketone **3** tentatively being most reactive. Experiments with the related derivatives 1′-oxomethyleugenol and (*E*)-3′-oxomethylisoeugenol revealed that both compounds readily form adducts with glutathione in nonenzymatic incubations with 1′-oxomethyleugenol being the most reactive. Additionally, 1′-oxomethyleugenol, but not (*E*)-3′-oxomethylisoeugenol, formed protein adducts with cytosolic and microsomal protein as well as bovine serum albumin at concentrations >0.5 mg protein/mL (Gerlach, M., Kercher, S., Schliwka, M., Cartus, A. T., and Schrenk, D., unpublished results). Therefore, the amounts of oxo-compounds, in particular those of **2**, found in the time-course measurements and the determined formation rates may be higher due to the possible trapping of those compounds in microsomal incubations thus escaping from detection. Further oxidation of **5** or **7** to the corresponding carboxylic acids was not observed in any incubation.

The formation of the mono-*O*-demethylated compounds **10** and **11** was demonstrated by ^{1}H NMR spectroscopy and consistent UV spectra. The formation of **12** was assumed based on the retention time and UV spectrum but not via NMR. However, a final assignment, whose peak represents one particular *O*-demethylated compound, notably a differentiation between **10** and **11**, cannot be made at present. No analytical hints to the formation of di- or tri-*O*-demethylated compounds in the incubations of liver microsomes with **1** were found.

Kinetic Parameters. On the basis of the results of the apparent time course measurements, an incubation time of 20 min was chosen for the determination of kinetic parameters since this is a good compromise between a desired short incubation time and a needed quantifiable yield of metabolites. The derivation of kinetic parameters was performed using the Michaelis−Menten or Hill equation by the criteria described in the Experimental Procedures section or were determined for the low K_m site if an apparent biphasic reaction profile was observed. Apparent kinetic data were derived for primary microsomal metabolites (side-chain alcohols **2** + **4** + **6**, and *O*-demethylated metabolites **10** + **11** + **12**) as well as for the secondary metabolites (diols **9a** + **9b**, ketone **13**, and **5** + **7**). In the case of diols **9a** + **9b** and ketone **13**, the determination of kinetic data via curve fitting was of good statistical quality. For the mono-*O*-demethylated compounds (**10** + **11** + **12**), parameter estimation was less stringent for rat liver microsomes, which formed quantifiable amounts at the highest substrate concentration only but were good for the other investigated liver microsomes. In the case of **5** + **7**, quantifiable amounts were just detectable in Aroclor 1254-pretreated rat liver microsomes after 20 min. It should be noted, that the apparent kinetic parameters for the sum of **5** + **7**, for the sum of **9a** + **9b**, and for ketone **13** bear a number of uncertainties since they were determined with a multienzyme mixture (liver microsomes) and because they are secondary metabolites, which means that the actual start concentration of the primary metabolites was unknown. Thus, the Hill coefficient n_H in the liver microsomal incubations will not be interpreted as a quantitative parameter for positive or negative cooperativity but rather referred to as an unspecified apparent correction term. However, in the case of the diols **9a** + **9b** and ketone **13**, the hydrolysis or formation was so fast that these values can be considered as sufficient surrogates for true kinetic parameters of formation of the epoxides **8a**/**8b**. The %-values of V_{max} and V_{max}/K_m are hence additive, and their sum can be interpreted tentatively as the total epoxide formation.

The kinetic data show clearly that the epoxidation of the side-chain (leading to diols **9a** and **9b** and ketone **13**) is by far the major metabolic route of the metabolism of **1** in all investigated liver microsomes. Furthermore, the data imply that the relative formation rates among metabolites are little or not dependent on substrate concentration for Aroclor 1254-pretreated rat, rat, bovine, and human liver microsomes. The only exception was porcine liver microsomes, for which a more dominant metabolic route via O-demethylation at low substrate concentrations was assumed. The ranking of total metabolite formation in terms of V_{max}/K_m was Aroclor 1254-pretreated rat liver microsomes > bovine liver microsomes > rat liver microsomes > porcine liver microsomes > human liver microsomes. In terms of total V_{max}, rat liver microsomes were most active, and the other investigated liver microsomes showed total V_{max} values in a similar range each under the given (initial rate) conditions. The finding of a higher apparent activity in terms of V_{max} of noninduced rat liver microsomes compared to Aroclor 1254-pretreated rat and other liver microsomes in the metabolism of **1** was somewhat unusual because of their lower P450 content. This may be due to a stronger induction of P450s with low k_{cat} and low K_m values than of P450s with high k_{cat} but also high K_m values by Aroclor 1254.

DOI: 10.1021/acs.chemrestox.5b00223
Chem. Res. Toxicol. XXXX, XXX, XXX−XXX

Preliminary data derived using a variety of recombinant human P450s show that the P450s 1A2, 2C19, and 3A4 are the main enzymes involved in the metabolism of **1** (Cartus, A. T., and Schrenk, D., unpublished results).

General Discussion. In the presented work we uncovered the hepatic (and epoxide hydrolysis) metabolism of **1** in liver microsomes from different species including humans and determined its apparent kinetic parameters. Thereby, one aim was to get first insights into the mechanism of action of the bioactivation of **1**. The mechanism of action leading to the hepatocarcinogenicity of ***allylic*** phenylpropenes like methyleugenol or estragole is assumed to be the P450 catalyzed formation of an 1′-hydroxy alcohol, which is afterward sulfonated by sulfotransferases (SULT). After the loss of sulfate, the formed carbocation can bind to DNA and thus cause mutations and eventually tumors. The metabolism and the possible bioactivation of ***propenylic*** phenylpropenes, e.g., methylisoeugenol and anethole differ from the metabolism of ***allylic*** compounds. For example, propenylic phenylpropenes do not usually form 1′-hydroxy metabolites *in vitro* or *in vivo*. Main reactions of those compounds are the formation of 3′-hydroxy metabolites, subsequent oxidation and β-oxidation thereof, as well as epoxidation of the side-chain and further hydrolysis.[18,28,39−42] For carcinogenic but nongenotoxic *trans*-anethole, its side-chain epoxide has been determined to be the ultimate hepatotoxic metabolite.[18,43,44] This epoxide can cause cytotoxicity and as a consequence regenerative hyperplasia in rat livers in the case of continuously elevated tissue concentrations of anethole.[18] In contrast to *trans*-anethole, **1** was found to be genotoxic, and metabolism is needed to activate the compound (cp. Introduction). Furthermore, carcinogenicity of **1** in mice seems to be rather not or not solely an effect of cytotoxicity induced by prolonged high concentrations of **1** since single or four time dosage design was used in these experiments.[13] This conclusion is supported by the nonregenerative pathological changes in the livers of rats orally treated with **1**.[14] So, the question is which metabolite(s) may be responsible for the genotoxic effects of **1**. Obvious candidates are 1′-hydroxyasarone (**2**) and the side-chain epoxide(s) **8a**/**8b**. Wiseman et al. showed that SULT-inhibition by pentachlorophenol (PCP) did not change the incidences of hepatomas in male mice treated with **1**.[13] Additionally, Hasheminejad and Caldwell showed that inhibition of P450 enzymes by cimetidine resulted in a lower genotoxicity of **1** in primary rat hepatocytes (measured as unscheduled DNA synthesis), but PCP was without effect.[21] Thus, although we detected the allylic alcohol **2** to be a minor metabolite of **1** in Aroclor 1254-pretreated rat liver microsomes, the mentioned results make it unlikely that the formation of **2** or another side-chain alcohol (**4** or **6**) is the crucial bioactivation step for **1**. Also, further experiments showed no evidence for a mutagenic activity of **2**, **4**, and **6** in a modified Ames test using (different) strains of *Salmonella thyphimurium* expressing different SULT isoforms (Berg, K., Wahl, A., Bischoff, R., Cartus, A. T., Glatt, H., and Schrenk, D., unpublished results). Already in the late 20th century, Elizabeth and James Miller hypothesized that side-chain epoxides may be responsible for the carcinogenicity of propenylic phenylpropenes such as α- and β-asarone.[38] Although at this time, nothing was known about the metabolism of asarone isomers, they investigated the mutagenicity and carcinogenicity of synthesized *trans*-asarone-epoxide (**8a**). Despite its low half-life in aqueous solutions, they found **8a** to be mutagenic in the Ames test (TA98 and TA100) and hepatocarcinogenic to young male B6C3F$_1$ mice (0.5 μmol/g body wt, ip). A similar mode of action for the *cis*-configurated epoxide **8b**, which is highly likely the main or only epoxide formed from **1** by liver microsomes, is reasonable. Experiments to elucidate the DNA binding properties of synthetic **8a**/**8b**, as well as the formation of DNA adducts in incubations of primary rat hepatocytes with **1**, are ongoing in our group. We do have strong LC-MS/MS-spectrometric evidence for the formation of a β-asarone-epoxide derived DNA-adduct, at least with deoxyguanosine (Stegmüller, S., Cartus, A. T., and Schrenk, D., unpublished results).

Taken together, our results support the hypothesis that the unstable and thus probably highly reactive epoxides **8a**/**8b** are the ultimate carcinogens of **1**. P450 enzymes are necessary for the activation of **1**, and both, microsomal and cytosolic epoxide hydrolases (EH), may be the predominant routes for enzymatic deactivation of the formed epoxide(s). The most meaningful hepatocarcinogenicity studies of **1** were performed in mice,[13] which in general show higher P450 activities and up to 35 times lower (microsomal) EH activities compared to those of humans. This may be taken into account with regard to a quantitative risk assessment of **1** (e.g., in foodstuffs) for humans.

■ ASSOCIATED CONTENT

Supporting Information

The Supporting Information is available free of charge on the ACS Publications website at DOI: 10.1021/acs.chemrestox.5b00223.

Detailed and full scale ^{1}H NMR spectra of the supernatants of microsomal incubations with **1**; secondary metabolism of asarone side-chain alcohols **2**, **4**, and **6**; selected HPLC-DAD chromatograms of the time course measurements; formation of ketone **13** and percentage of *erythro*-diol **9b** in spontaneous hydrolysis experiments with **8a** and **8b**; Michaelis−Menten, Hill, and Eadie-Hofstee plots; ^{1}H- and ^{13}C-{^{1}H}-NMR spectra of the synthesized compounds (PDF)

■ AUTHOR INFORMATION

Corresponding Author

*Phone: +49-0-631 205 3217. Fax: +49-0-631 205 4398. E-mail: schrenk@rhrk.uni-kl.de.

Funding

This work was funded by the German Research Foundation (Deutsche Forschungsgemeinschaft, DFG) under grant #SCHR 327/14-1.

Notes

The authors declare no competing financial interest.

■ ACKNOWLEDGMENTS

We thank Hans-Joachim Schmitz for providing rat livers. The provision of bovine liver microsomes by the team of Gerhard Eisenbrand at the University of Kaiserslautern is gratefully acknowledged. We also thank Melanie Beckmann for expert technical assistance.

■ ABBREVIATIONS

1, β-asarone ((*Z*)-2,4,5-trimethoxy-1-propenylbenzene, CAS No. 5273-86-9); **2**, 1′-hydroxyasarone (CAS No. 1517851-36-3); **3**, 1′-oxoasarone (CAS No. 1500937-73-4); **4**, (*E*)-3′-hydroxyasarone (CAS No. 1392497-89-0); **5**, (*E*)-3′-oxoasarone (CAS No. 99217-06-8); **6**, (*Z*)-3′-hydroxyasarone (CAS No. 1402544-70-0); **7**, (*Z*)-3′-oxoasarone (CAS No. 99217-07-9);

DOI: 10.1021/acs.chemrestox.5b00223
Chem. Res. Toxicol. XXXX, XXX, XXX−XXX

8a, (*E*)-asarone-1′,2′-epoxide (CAS No. 124878-08-6); **8b**, (*Z*)-asarone-1′,2′-epoxide (CAS No. 321365-66-6); **9a**, *threo*-1′,2′-dihydrodihydroxy-asarone (CAS No. 146830-05-9); mixture of (1*R*,2*R*)- and (1*S*,2*S*)-1-(2,4,5-trimethoxyphenyl)-propane-1,2-diol (CAS No. 321365-67-7 relative configuration, 853021-83-7 absolute configuration, and 137361-00-3 relative configuration, 853021-82-6 absolute configuration, respectively); **9b**, *erythro*-1′,2′-dihydrodihydroxy-asarone (CAS No. 146830-05-9); mixture of (1*S*,2*R*)- and (1*R*,2*S*)-1-(2,4,5-trimethoxyphenyl)-propane-1,2-diol (CAS No. 137361-02-5 relative configuration, 853021-85-9 absolute configuration, and 321365-68-8 relative configuration, 853021-84-8 absolute configuration); **10**, 3-hydroxyasarone (no CAS No. assigned); **11**, 4-hydroxyasarone (no CAS No. assigned); **12**, (*Z*)-6-hydroxyasarone (CAS No. 65720-04-9); **13**, 2,4,5-trimethoxyphenylacetone (CAS No. 2020-90-8); **14**, 3,4-dimethoxypropylbenzene (CAS No. 5888-52-8); DAD, diode array detector; DMSO, dimethyl sulfoxide (Me_2SO); PCP, pentachlorophenol

REFERENCES

(1) Rana, T. S., Mahar, K. S., Pandey, M. M., Srivastava, S. K., and Rawat, A. K. (2013) Molecular and chemical profiling of 'sweet flag' (*Acorus calamus* L.) germplasm from India. *Physiol. Mol. Biol. Plants 19*, 231−237.

(2) Satyal, P., Paudel, P., Poudel, A., Dosoky, N. S., Moriarity, D. M., Vogler, B., and Setzer, W. N. (2013) Chemical compositions, phytotoxicity, and biological activities of Acorus calamus essential oils from Nepal. *Nat. Prod. Commun. 8*, 1179−1181.

(3) Rajput, S. B., Tonge, M. B., and Karuppayil, S. M. (2014) An overview on traditional uses and pharmacological profile of *Acorus calamus* Linn. (Sweet flag) and other *Acorus* species. *Phytomedicine 21*, 268−276.

(4) Mukherjee, P. K., Kumar, V., Mal, M., and Houghton, P. J. (2007) Acorus calamus: Scientific Validation of Ayurvedic Tradition from Natural Resources. *Pharm. Biol. 45*, 651−666.

(5) Mukherjee, P. K., Kumar, V., Mal, M., and Houghton, P. J. (2007) *In vitro* Acetylcholinesterase Inhibitory Activity of the Essential Oil from *Acorus calamus* and its Main Constituents. *Planta Med. 73*, 283−285.

(6) Mukherjee, P. K., Rai, S., Kumar, V., Mukherjee, K., Hylands, P., and Hider, R. (2007) Plants of Indian origin in drug discovery. *Expert Opin. Drug Discovery 2*, 633−657.

(7) Björnstad, K., Helander, A., Hultén, P., and Beck, O. (2009) Bioanalytical Investigation of Aasarone in Connection with *Acorus calamus* Oil Intoxications. *J. Anal. Toxicol. 33*, 604−609.

(8) Schultes, R. E. (1976) *Hallucinogenic Plants, illus. Smith, E.W.*, Golden Press, New York.

(9) Hoffer, A., and Osmond, H. (1967) *The Hallucinogens*, Academic Press Inc., New York.

(10) Fang, Y. Q., Shi, C., Liu, L., and Fang, R. M. (2012) Analysis of transformation and excretion of *β*-asarone in rabbits with GC-MS. *Eur. J. Drug Metab. Pharmacokinet. 37*, 187−190.

(11) Fang, Y. Q., Shi, C., Liu, L., and Fang, R. M. (2012) Pharmacokinetics of *β*-asarone in rabbit blood, hippocampus, cortex, brain stem, thalamus and cerebellum. *Pharmazie 67*, 120−123.

(12) Meng, X., Zhao, X., Wang, S., Jia, P., Bai, Y., Liao, S., and Zheng, X. (2013) Simultaneous Determination of Volatile Constituents from *Acorus tatarinowii* Schott in Rat Plasma by Gas Chromatography-Mass Spectrometry with Selective Ion Monitoring and Application in Pharmacokinetic Study. *J. Anal. Methods Chem. 2013*, 1−7.

(13) Wiseman, R. W., Miller, E. C., Miller, J. A., and Liem, A. (1987) Structure-Activity Studies of the Hepatocarcinogenicities of Alkenylbenzene Derivatives Related to Estragole and Safrole on Administration to Preweanling Male C57BL/6J × C3H/HeJ F_1 mice. *Cancer Res. 47*, 2275−2278.

(14) JECFA (Joint FAO/WHO Expert Committee on Food Additives) (1981) *Toxicological Evaluation of Certain Food Additives*, WHO Technical Report Series No. 669, pp 33−44, WHO, Geneva, Switzerland.

(15) van den Berg, S. J., Restani, P., Boersma, M. G., Delmulle, L., and Rietjens, I. M. (2011) Levels of Genotoxic and Carcinogenic Compounds in Plant Food Supplements and Associated Risk Assessment. *Food Nutr. Sci. 2*, 989−1010.

(16) Taylor, J. M., Jones, W. I., Hagan, E. C., Gross, M. A., Davis, D. A., and Cook, E. L. (1967) Toxicity of oil of calamus (Jammus variety). *Toxicol. Appl. Pharmacol. 10*, 405.

(17) SCF (Scientific Committee on Food) (2002) Opinion of the Scientific Committee on Food on the Presence of *β*-Asarone in Flavourings and Other Food Ingredients with Flavouring Properties, SCF/CS/FLAV/FLAVOUR/9 ADD1 Final, available online at http://ec.europa.eu/food/fs/sc/scf/out111_en.pdf.

(18) Newberne, P., Smith, R. L., Doull, J., Goodman, J. I., Munro, I. C., Portoghese, P. S., Wagner, B. M., Weil, C. S., Woods, L. A., Adams, T. B., Lucas, C. D., and Ford, R. A. (1999) The FEMA GRAS assessment of trans-anethole used as a flavouring substance. Flavour and Extract Manufacturer's Association. *Food Chem. Toxicol. 37*, 789−811.

(19) Göggelmann, W., and Schimmer, O. (1983) Mutagenicity testing of *β*-asarone and commercial calamus drugs with *Salmonella typhimurium*. *Mutat. Res. Lett. 121*, 191−194.

(20) Abel, G., and Göggelmann, W. (1986) Genotoxic activity of *β*-asarone and commercial calamus drugs. *Mutat. Res., Environ. Mutagen. Relat. Subj. 164*, 287.

(21) Hasheminejad, G., and Caldwell, J. (1994) Genotoxicity of the Alkenylbenzenes *α*- and *β*-Asarone, Myristicin and Elimicin as Determined by the UDS Assay in Cultured Rat Hepatocytes. *Food Chem. Toxicol. 32*, 223−231.

(22) Kevekordes, S., Spielberger, J., Burghaus, C. M., Birkenkamp, P., Zietz, B., Paufler, P., Diez, M., Bolten, C., and Dunkelberg, H. (2001) Micronucleus Formation in Human Lymphocytes and in the Metabolically Competent Human Hepatoma Cell Line Hep-G2: Results with 15 Naturally Occurring Substances. *Anticancer Res. 21*, 461−469.

(23) Unger, P., and Melzig, M. F. (2012) Comparative Study of the Cytotoxicity and Genotoxicity of Alpha- and Beta-Asarone. *Sci. Pharm. 80*, 663−668.

(24) Abel, G. (1987) Chromosome Damaging Effect on Human Lymphocytes by *β*-Asarone /Chromosomenschädigende Wirkung von beta-Asaron in menschlichen Lymphocyten. *Planta Med. 53*, 251−253.

(25) 21CFR189, Code of Federal Regulations (2003) *Title 21: Food and Drugs: Chapter I: Food and Drug Administration, Department of Health and Human Services (Continued) Part 189: Substances Prohibited from Use in Human Food*, Vol. 3, pp 571−572, Food and Drug Administration, Washington, DC.

(26) Regulation (EC) No. 1334/2008 of the European Parliament and of the Council of 16 December 2008 on Flavourings and Certain Food Ingredients with Flavouring Properties for Use in and on Foods and Amending Council Regulation (EEC) No 1601/91, Regulations (EC) No. 2232/96 and (EC) No. 110/2008 and Directive 2000/13/EC, available online at http://eur-lex.europa.eu/legal-content/EN/TXT/?uri=celex:32008R1334.

(27) COE (Committee of Experts on Flavouring Substances of the Council of Europe) (2005) The 1st Report on Active Principles (Constituents of Toxicological Concern) Contained in Natural Sources of Flavourings, available online at http://www.coe.int/t/e/social_cohesion/soc%2Dsp/public_health/flavouring_substances/Active%20principles.pdf.

(28) Cartus, A. T., Merz, K. H., and Schrenk, D. (2011) Metabolism of Methylisoeugenol in Liver Microsomes of Human, Rat, and Bovine Origin. *Drug Metab. Dispos. 39*, 1727−1733.

(29) Melancon, M. J., Williams, D. E., Buhler, D. R., and Lech, J. J. (1985) Metabolism of 2-Methylnaphthalene by Rat and Rainbow Trout Hepatic Microsomes and Purified Cytochromes P-450. *Drug Metab. Dispos. 13*, 542−547.

(30) Bradford, M. M. (1976) A Rapid and Sensitive Method for the Quantitation of Microgram Quantities of Protein Utilizing the Principle of Protein-Dye Binding. *Anal. Biochem. 72*, 248−254.

DOI: 10.1021/acs.chemrestox.5b00223
Chem. Res. Toxicol. XXXX, XXX, XXX−XXX

(31) Omura, T., and Sato, R. (1962) A new Cytochrome in Liver Microsomes. *J. Biol. Chem. 239*, 2370−2385.
(32) Hutzler, J. M., and Tracy, T. S. (2002) Atypical Kinetic Profiles in Drug Metabolism Reactions. *Drug Metab. Dispos. 30*, 355−362.
(33) Soars, M. G., Ring, B. J., and Wrighton, S. A. (2003) The Effect of Incubation Conditions on the Enzyme Kinetics of UDP-Glucuronosyltransferases. *Drug Metab. Dispos. 31*, 762−767.
(34) Sono, M., Roach, M. P., Coulter, E. D., and Dawson, J. H. (1996) Heme-Containing Oxygenases. *Chem. Rev. 96*, 2841−2888.
(35) Chiappe, C., De Rubertis, A., Amato, G., and Gervasi, P. G. (1998) Stereochemistry of the Biotransformation of 1-Hexene and 2-Methyl-1-hexene with Rat Liver Microsomes and Purified P450s of Rats and Humans. *Chem. Res. Toxicol. 11*, 1487−1493.
(36) Chiappe, C., De Rubertis, A., De Carlo, M., Amato, G., and Gervasi, P. G. (2001) Stereochemical Aspects in the 4-Vinylcyclohexene Biotransformation with Rat Liver Microsomes and Purified P450s. Monoepoxides and Diols. *Chem. Res. Toxicol. 14*, 492−499.
(37) Mohan, R. S., Gavardinas, K., Kyere, S., and Whalen, D. L. (2000) Spontaneous Hydrolysis Reactions of *cis*- and *trans*-β-Methyl-4-methoxystyrene Oxides (Anethole Oxides): Buildup of *trans*-Anethole Oxide as an Intermediate in the Spontaneous Reaction of *cis*-Anethole Oxide. *J. Org. Chem. 65*, 1407−1413.
(38) Kim, S. G., Liem, A., Stewart, B. C., and Miller, J. A. (1999) New studies on *trans*-anethole oxide and *trans*-asarone oxide. *Carcinogenesis 20*, 1303−1307.
(39) Solheim, E., and Scheline, R. R. (1976) Metabolism of Alkenebenzene Derivatives in the Rat. II. Eugenol and Isoeugenol Methyl Ethers. *Xenobiotica 6*, 137−150.
(40) Solheim, E., and Scheline, R. R. (1973) Metabolism of Alkenebenzene Derivatives in the Rat. I. *p*-Methoxyallylbenzene (Estragole) and *p*-Methoxypropenylbenzene (Anethole). *Xenobiotica 3*, 493−510.
(41) Solheim, E., and Scheline, R. R. (1980) Metabolism of lkenebenzene derivatives in the rat. III. Elemicin and isoelemicin. *Xenobiotica 10*, 371−380.
(42) Rietjens, I. M., Cohen, S. M., Fukushima, S., Gooderham, N. J., Hecht, S., Marnett, L. J., Smith, R. L., Adams, T. B., Bastaki, M., Harman, C. G., and Taylor, S. V. (2014) Impact of structural and metabolic variations on the toxicity and carcinogenicity of hydroxy- and alkoxy-substituted allyl- and propenylbenzenes. *Chem. Res. Toxicol. 27*, 1092−1103.
(43) Howes, A. J., Chan, V. S., and Caldwell, J. (1990) Structure-specificity of the genotoxicity of some naturally occurring alkenylbenzenes determined by the unscheduled DNA synthesis assay in rat hepatocytes. *Food Chem. Toxicol. 28*, 537−542.
(44) Gorelick, N. J. (1995) Genotoxicity of *trans*-anethole *in vitro*. *Mutat. Res., Fundam. Mol. Mech. Mutagen. 326*, 199−209.

DOI: 10.1021/acs.chemrestox.5b00223
Chem. Res. Toxicol. XXXX, XXX, XXX−XXX